

Aggregation-Induced Emission of Hexaphenyl-1,3-butadiene

Yahui Zhang,^a Lingwei Kong,^a Jianbing Shi,^{*,a} Bin Tong,^a Junge Zhi,^b
Xiao Feng,^b and Yuping Dong^{*,a}

^a School of Materials Science and Engineering, Beijing Institute of Technology, Beijing 100081, China

^b School of Chemistry, Beijing Institute of Technology, Beijing 100081, China

A new type of AIE molecules based on hexaphenyl-1,3-butadienes was reported with respect to the synthesis and characterization. This material exhibited different maximum emission wavelength and enhanced emission intensity at different aggregate state (amorphous and crystalline state).

Keywords aggregation-induced emission, hexaphenyl-1,3-butadienes, aggregate state, phase transition

Introduction

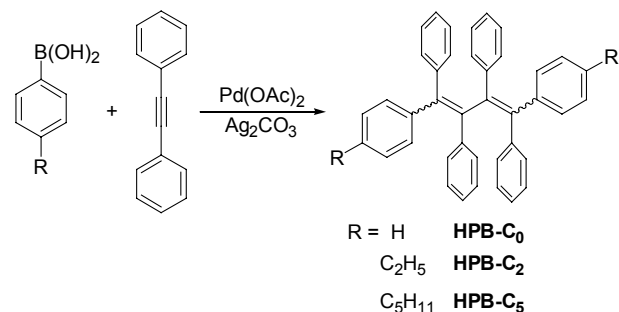
The development of organic luminescent materials is of significance due to their important applications in fluorescent sensors and light-emitting diode fabrication.^[1] In recent years, some luminogenic materials were found emitting more efficiently in the form of film than in solution and have received considerable interest. As one of the typical examples, the emission of silole molecules was first demonstrated to be stronger in the aggregate state than that in the solution state by Tang *et al.* in 2001.^[2] A concept of aggregation-induced emission (AIE) was coined accordingly for the unusual phenomenon in the aggregate state. Such a novel effect has enabled the AIE luminogens to find potential high-tech applications in sensors and opto-electrical devices over the past years.^[3]

Most AIE molecules share some common features such as propeller-like structures with some rotors. Both experimental results and theoretical calculations have indicated that the AIE mechanism of those AIE luminogens is to block the radiationless relaxation channel and open the radiative decay pathway because the rotations of the rotors are restricted due to the involved physical constraint in the aggregate state.^[4] So the compounds with a more twisted configuration can efficiently prevent parallel orientation of conjugated chromophores and strengthen the restricted intramolecular rotation (RIR) effect. Under the guidance of the mechanism understanding, researchers have designed and synthesized a large variety of AIE molecules, including hydrocarbon system,^[5] heteroatom system,^[6] organometallic system,^[7] and so on. The exploitation and design of new AIE molecules remain a promising direction in this exciting area given their fundamental importance and practical

applications.

In our previous report, aryl-substituted 1,3-butadiene derivatives proved excellent candidates for AIE chromophores with simple synthesis and outstanding mechanochromic behavior.^[8] If two hydrogen atoms in the positions 2 and 3 in tetra-aryl substituted 1,3-butadiene derivatives can be substituted by aryl groups, we speculated the target substances should enhance the AIE properties and deepen the understanding of the AIE mechanism. In this report, three hexaphenyl-1,3-butadiene (HPB) derivatives without and with the different alkyl groups were synthesized by a one-step reaction under mild conditions according to the reference^[9] as shown in Scheme 1. All compounds were purified and characterized by standard spectroscopic techniques including NMR, MS and elemental analysis, see supplementary information.

Scheme 1 Synthetic routes of HPB-C_x



Results and Discussion

Three compounds are soluble in common organic solvents such as dichloromethane and tetrahydrofuran (THF) but insoluble in water. Therefore, AIE features of

* E-mail: bing@bit.edu.cn; chdongyp@bit.edu.cn; Tel.: 0086-10-68917390; Fax: 0086-10-68917390

Received February 6, 2015; accepted May 20, 2015; published online June 2, 2015.

Supporting information for this article is available on the WWW under <http://dx.doi.org/10.1002/cjoc.201500116> or from the author.

HPB-C_x were studied by measuring the change in their fluorescence intensity in THF-water mixtures as plotted in Figure S1 (see SI). The correlation between the net change in the maximum PL intensities of **HPB-C_x** and the water fraction (f_w) is shown in Figure 1. The fluorescence intensities of their THF solution with an f_w lower than 60% were negligibly small. This is due to the non-radiative decay caused by the free intramolecular rotation of the σ bonds between phenyl and alkenyl. The emission began to drastically increase once the f_w reached 70%, at which point, the aggregates started to form because the transmittance of **HPB-C_x** distinctly decreased at high water contents ($\geq 70\%$). This indicated that the molecules of **HPB-C_x** have clustered into larger size of the aggregates, as shown in Figure S2 (SI), and the free rotations were restricted. With an f_w of 90%, the PL intensities of **HPB-C₀**, **HPB-C₂** and **HPB-C₅** were increased by ~14, 12 and 17 fold, respectively. The dynamic light scattering (DLS) confirmed the aggregate formation, and their particle diameter sizes of **HPB-C₀**, **HPB-C₂** and **HPB-C₅** were 330, 303 and 234 nm, respectively, when f_w reached 70% (Figure S3 in SI). Evidently, the enhanced emission intensity of **HPB-C_x** is spectacularly boosted by the aggregation. In other words, **HPB-C_x** is AIE active. Moreover, alkyl chains show little effect on the AIE performance although increased times of fluorescence intensity have slightly different values.

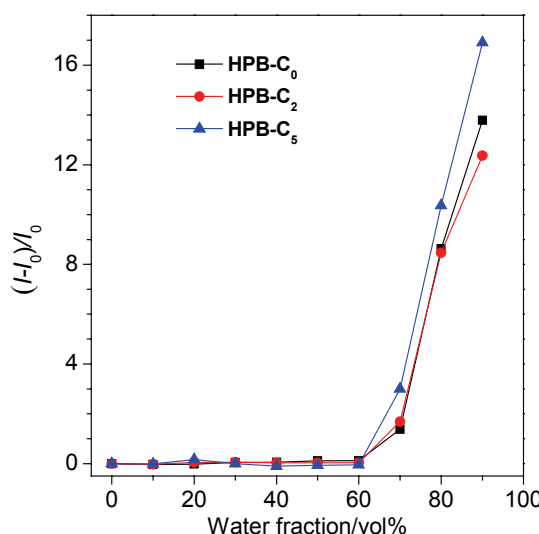


Figure 1 Correlation between the net change in PL intensity $[(I-I_0)/I_0]$ of **HPB-C₀**, **HPB-C₂** and **HPB-C₅** at 490 nm without (I_0) and with different water fractions in the THF/water mixtures. $[HPB-C_x]=7\times 10^{-5}$ mol/L; Excitation wavelength: 360 nm.

The crystal structure of the chromophores is the direct evidence we can utilize to know the arrangement of the AIE molecules in the solid state, which is helpful for the understanding of the AIE mechanism. Single crystals of **HPB-C_x** were grown through their slow crystallization in a CH_2Cl_2 solvent. But only the single crystal

of **HPB-C₀** was successfully obtained. We attempted other solvents and/or methods for **HPB-C₂** and **HPB-C₅** but failed. This is probably due to the existence of alkyl groups resulting to different stereoisomers such as *Z-Z*, *Z-E* and *E-E* isomers, which are unfavorable for the highly ordered alignment of molecules. Crystal of **HPB-C₀** with high quality was used for the single-crystal X-ray crystallography (SXRD) analysis. As shown in Figure 2A, **HPB-C₀** adopts a highly twisted conformation, which had a helical structure for the backbone of the butadiene. In addition, there are large torsion angles between the ethylenic group and the phenyl group of 47.10° , 44.77° , 33.91° , 61.77° , 38.33° and 64.26° for $\theta_1-\theta_6$, respectively. This indicated that any phenyl groups in **HPB-C₀** molecule can freely rotate in solvents and thus consume the exciton energies and make **HPB-C₀** non-emissive in solutions. Upon aggregation, these intramolecular rotations are highly restricted and boost the emissive efficiency. Moreover, the dihedral angles between the adjacent phenyl rings are 56.35° , 69.88° , 63.91° , 82.85° , 17.22° and 86.86° for θ_{AB} , θ_{BC} , θ_{CD} , θ_{DE} , θ_{EF} and θ_{FA} , respectively. And the crystal packing of the adjacent **HPB-C₀** molecules is mainly edge-to-face interactions such as aromatic $\text{CH}\cdots\pi$ interactions and hardly formed $\pi\cdots\pi$ interactions. Their distances are found to be 2.923 Å and 3.323 Å as shown in Figure 2C. The interactions of the aromatic $\text{CH}\cdots\pi$ in turn stabilize the twisted conformation of the molecules, which is in favor of hindering the rotation of the single bond between phenyl rings and ethylenic group and minimizes the possibility of forming excimers in the crystal. These results demonstrate that the formation of aggregates imposes physical restraints on the intramolecular rotations, and thus blocks the radiationless relaxation channel and opens the radiative decay pathway.

Thermal stability of the **HPB-C_x** was evaluated by thermo gravimetric analysis (TGA) under nitrogen. As shown in Figure S4 (SI), the decomposition temperatures (T_d) of these three compounds range from 268 to 288 °C, demonstrating that all compounds are thermally stable. A good thermal stability is required for future device applications. Moreover, the melting points of these three compounds are 204.4, 183.0 and 116.0 °C, respectively, far lower than T_d . So we quenched the melted samples using liquid nitrogen to obtain the amorphous state because we found that **HPB-C₀** tends to crystallize. It is interesting to note the difference between the crystal and amorphous states although both of them belong to the aggregated state. Powder X-ray diffraction (PXRD) was performed to track the phase state. As shown in Figure 3A, the PXRD pattern of **HPB-C₀** in single crystal (**HPB-C₀-1**) showed multiple peaks while almost no peak was observed for amorphous state (**HPB-C₀-2**). Correspondingly, the maximum emission wavelength of **HPB-C₀** in amorphous state (red in Figure 3B) is shifted to 493 nm from 471 nm in single crystal. In the above discussion about the aggregate

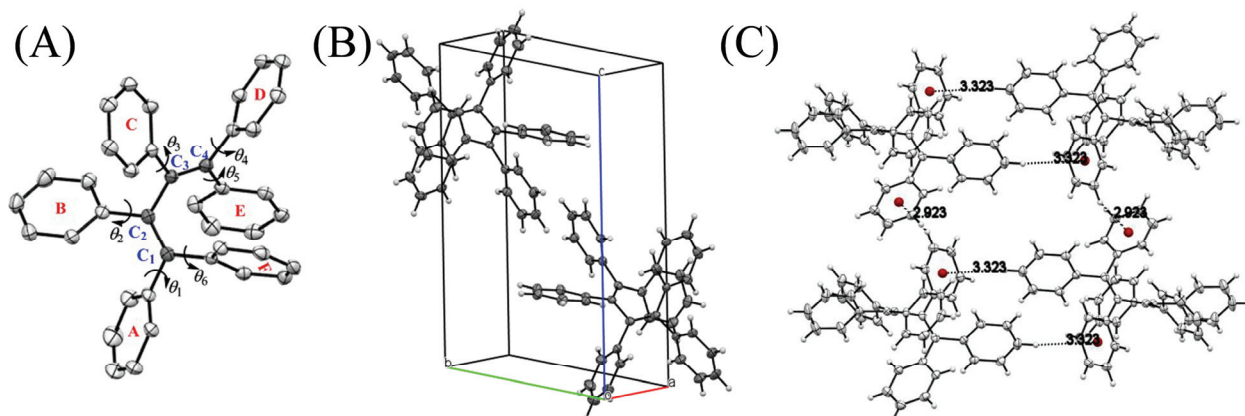


Figure 2 (A) ORTEP drawing of single-crystal structure of **HPB-C₀** (deletion of the hydrogen atom for clarity); (B) packing structure of **HPB-C₀** single crystal and (C) intermolecular interactions of **HPB-C₀**.

formation of **HPB-C₀** in mixture solution by addition of non-solvent, its maximum emission wavelengths are about 480, 486 and 488 nm when the f_{ws} reach 70%, 80% and 90%, respectively. So the aggregate state in the mixture solution consists of amorphous state or a mixture of amorphous and crystalline states, that is, loose alignment is formed when the molecules of **HPB-C₀** are forced to rapidly aggregate. It is straightforward to understand because the formation of the aggregates was too fast to regularly arrange when a large amount of water was added into the THF solution. But amorphous **HPB-C₀** can re-crystallize by fuming with dichloromethane vapour. The sharp diffraction peaks in its PXRD pattern (**HPB-C₀-3** in Figure 3A) appear again, that is, the crystalline state can be recovered. In addition, the maximum emission wavelength also returned to 471 nm (blue in Figure 3B). What is more interesting, the emission intensity of **HPB-C₀** is gradually enhanced with the extended exposure time of fumigation, as shown in Figure S5. To better understand the unique PL behaviors of **HPB-C₀** in crystalline and amorphous states, we studied their UV-Vis absorption spectra by the assistance of integrating sphere. In order to compare the difference, the spectra are normalized and shown in Figure S6. The small red-shift was observed for amorphous states, which is consistent with the above PL results. Additionally, the quantum yield (Φ) is an important parameter for a chromophore, and the emission efficiency can be quantitatively evaluated accordingly. The absolute PL quantum yields of **HPB-C₀** in both amorphous and crystalline states were determined by using an integrating sphere. The Φ values of **HPB-C₀** in crystalline and amorphous states were 3.53% and 2.42%, respectively. These result indicated that the more compact aggregates, the more efficient emission. On the other hand, these results demonstrated that the AIE mechanism is mainly due to RIR. We also investigated the reversibility between amorphous and crystalline state, as shown in Figure S7 where the reproducibility maintains well after four melting-freezing-fuming cycles. Their maximum emission wavelengths (λ_{max})

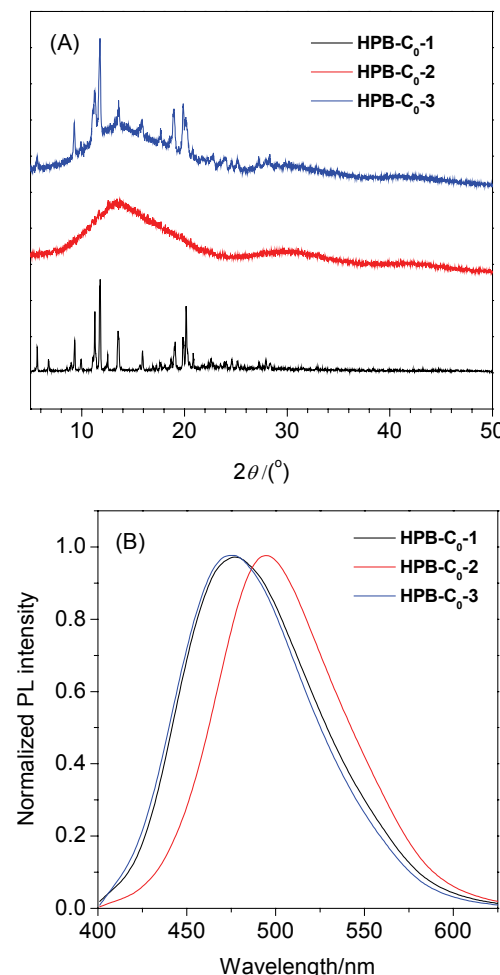


Figure 3 (A) PXRD patterns and (B) normalized PL spectra of the **HPB-C₀** at different states. **1**—single crystal; **2**—amorphous; **3**—crystal obtained from amorphous state by CH₂Cl₂ vapor fuming. The excitation wavelength is at 360 nm.

change reversibly between 471 and 494 nm with almost no deterioration, indicating the excellent reversibility of its aggregate state. Compared with photoluminescence properties of **HPB-C₀**, the AIE characteristics are observed in **HPB-C₂** and **HPB-C₅**, too (Figure 1). The

fluorescence intensities of the two compounds in amorphous state, however, persistently decrease with the increasing of fumigation time in the dichloromethane vapor until 190 s and then almost unchangeable (Figure S5 in SI). We speculated that the formation of the regular aggregation induced by dichloromethane vapor is very slow or difficult due to the steric hindrance induced by alkyl group.

Conclusions

In summary, we successfully synthesized and characterized a new series of AIE-active dyes of hexaphenyl-1,3-butadienes. The RIR process is the predominant mechanism for the AIE effects. The results imply that this is an effective molecular strategy to design new AIE materials. It is also anticipated that more amazing AIE chromophores based on HPB can be designed with the introduction of diversified functional groups, which may help us realize a better understanding of AIE phenomenon, mechanism, and application.

Acknowledgement

This work was financially supported by the National Natural Science Foundation of China (Grant Nos. 21474009, 51328302, 51073026, 51061160500), the National Basic Research Program of China (973 Program; Grant No. 2013CB834704) and Basic Research Foundation of Beijing Institute of Technology (Grant No. 20130942007).

References

- [1] (a) Zhou, Y.; He, Q. G.; Yang, Y.; Zhong, H. Z.; He, C.; Sang, G. Y.; Liu, W.; Yang, C. H.; Bai, F. L.; Li, Y. F. *Adv. Funct. Mater.* **2008**, *18*, 3299; (b) Bunz, U. H. F. *Chem. Rev.* **2000**, *100*, 1605; (c) Duarte, A.; Pu, K. Y.; Liu, B.; Bazan, G. C. *Chem. Mater.* **2011**, *23*, 501; (d) Wan, W.; Du, H. L.; Wang, J.; Le, Y. P.; Jiang, H. Z.; Chen, H.; Zhu, S. Z.; Hao, J. *Dyes Pigm.* **2013**, *96*, 642; (e) Rochat, S.; Swager, T. M. *ACS Appl. Mater. Interfaces* **2013**, *5*, 4488; (f) Chen, D. C.; Zhou, H.; Li, X. C.; Liu, M.; Ye, H.; Su, S. J.; Cao, Y. *Org. Electron.* **2014**, *15*, 1197; (g) Li, K.; Liu, B. *Chem. Soc. Rev.* **2014**, *43*, 6570; (h) Feng, G. X.; Liu, J.; Zhang, R. Y.; Liu, B. *Chem. Commun.* **2014**, *50*, 9497.
- [2] (a) Luo, J. D.; Xie, Z. L.; Lam, J. W. Y.; Cheng, L.; Chen, H. Y.; Qiu, C. F.; Kwok, H. S.; Zhan, X. W.; Liu, Y. Q.; Zhu, D. B.; Tang, B. Z. *Chem. Commun.* **2001**, *1740*; (b) Hong, Y.; Lam, J. W. Y.; Tang, B. Z. *Chem. Commun.* **2009**, *4332*; (c) Hong, Y.; Lam, J. W. Y.; Tang, B. Z. *Chem. Soc. Rev.* **2011**, *40*, 5361; (d) Mei, J.; Hong, Y.; Lam, J. W. Y.; Qin, A.; Tang, Y.; Tang, B. Z. *Adv. Mater.* **2014**, *26*, 5429.
- [3] (a) Hong, Y.; Xiong, H.; Lam, J. W. Y.; Haeussler, M.; Liu, J.; Yu, Y.; Zhong, Y.; Sung, H. H. Y.; Williams, I. D.; Wong, K. S.; Tang, B. Z. *Chem. Eur. J.* **2010**, *16*, 1232; (b) Xu, Y. H.; Chen, L.; Guo, Z. Q.; Nagai, A.; Jiang, D. L. *J. Am. Chem. Soc.* **2011**, *133*, 17622; (c) Luo, J.; Wang, X.; Wang, X.; Su, W. *Chin. J. Chem.* **2012**, *30*, 2488; (d) Zhang, X.; Zhang, X.; Yang, B.; Wang, S.; Liu, M.; Zhang, Y.; Tao, L.; Wei, Y. *RSC Adv.* **2013**, *3*, 9633; (e) He, B. R.; Ye, S. H.; Guo, Y. J.; Chen, B.; Xu, X. F.; Qiu, H. Y.; Zhao, Z. J. *Sci. China Chem.* **2013**, *56*, 1221; (f) Shi, J. B.; Wu, Y. M.; Sun, S.; Tong, B.; Zhi, J. G.; Dong, Y. P. *J. Polym. Sci. Part A-Polym. Chem.* **2013**, *51*, 229; (g)
- [4] (a) Chen, J. W.; Law, C. C. W.; Lam, J. W. Y.; Dong, Y. P.; Lo, S. M. F.; Williams, I. D.; Zhu, D. B.; Tang, B. Z. *Chem. Mater.* **2003**, *15*, 1535; (b) Tong, H.; Dong, Y.; Hong, Y.; Haussler, M.; Lam, J. W. Y.; Sung, H. H. Y.; Yu, X.; Sun, J.; Williams, I. D.; Kwok, H. S.; Tang, B. Z. *J. Phys. Chem. C* **2007**, *111*, 2287; (c) Zeng, Q.; Li, Z.; Dong, Y.; Di, C. A.; Qin, A.; Hong, Y.; Ji, L.; Zhu, Z.; Jim, C. K. W.; Yu, G.; Li, Q.; Li, Z.; Liu, Y.; Qin, J.; Tang, B. Z. *Chem. Commun.* **2007**, *70*; (d) Shi, J. Q.; Chang, N.; Li, C. H.; Mei, J.; Deng, C. M.; Luo, X. L.; Liu, Z. P.; Bo, Z. S.; Dong, Y. Q.; Tang, B. Z. *Chem. Commun.* **2012**, *48*, 10675.
- [5] (a) Tong, H.; Dong, Y. Q.; Haussler, M.; Lam, J. W. Y.; Sung, H. H. Y.; Williams, I. D.; Sun, J. Z.; Tang, B. Z. *Chem. Commun.* **2006**, *1133*; (b) Luo, X. L.; Li, J. N.; Li, C. H.; Heng, L. P.; Dong, Y. Q.; Liu, Z. P.; Bo, Z. S.; Tang, B. Z. *Adv. Mater.* **2011**, *23*, 3261; (c) Zhang, Z. Y.; Xu, B.; Su, J. H.; Shen, L. P.; Xie, Y. S.; Tian, H. *Angew. Chem., Int. Ed.* **2011**, *50*, 11654; (d) Li, Y. X.; Chen, Z.; Cui, Y.; Xia, G. M.; Yang, X. F. *J. Phys. Chem. C* **2012**, *116*, 6401; (e) Yang, L. J.; Ye, J. W.; Xu, L. F.; Yang, X. Y.; Gong, W. T.; Lin, Y.; Ning, G. L. *RSC Adv.* **2012**, *2*, 11529; (f) Li, C.; Luo, X.; Zhao, W.; Huang, Z.; Liu, Z.; Tong, B.; Dong, Y. *Sci. China Chem.* **2013**, *56*, 1173; (g) Dong, Y. F.; Wang, W. L.; Cewen, C. W.; Shi, J. B.; Tong, B.; Feng, X.; Zhi, J. G.; Dong, Y. P. *Tetrahedron Lett.* **2014**, *55*, 1496; (h) Zhang, G.-F.; Aldred, M. P.; Chen, Z.-Q.; Chen, T.; Meng, X.; Zhu, M.-Q. *RSC Adv.* **2015**, *5*, 1079.
- [6] (a) Li, Z.; Dong, Y. Q.; Lam, J. W. Y.; Sun, J. X.; Qin, A. J.; Haeussler, M.; Dong, Y. P.; Sung, H. H. Y.; Williams, I. D.; Kwok, H. S.; Tang, B. Z. *Adv. Funct. Mater.* **2009**, *19*, 905; (b) Shiraishi, K.; Kashiwabara, T.; Sanji, T.; Tanaka, M. *New J. Chem.* **2009**, *33*, 1680; (c) Feng, X.; Tong, B.; Shen, J.; Shi, J.; Han, T.; Chen, L.; Zhi, J.; Lu, P.; Ma, Y.; Dong, Y. *J. Phys. Chem. B* **2010**, *114*, 16731; (d) Bandrowsky, T. L.; Carroll, J. B.; Braddock-Wilking, J. *Organometallics* **2011**, *30*, 3559; (e) Han, T.; Feng, X.; Tong, B.; Shi, J.; Chen, L.; Zhi, J.; Dong, Y. *Chem. Commun.* **2012**, *48*, 416; (f) Dong, Y. J.; Xu, B.; Zhang, J. B.; Tan, X.; Wang, L. J.; Chen, J. L.; Lv, H. G.; Wen, S. P.; Li, B.; Ye, L.; Zou, B.; Tian, W. *J. Angew. Chem., Int. Ed.* **2012**, *51*, 10782; (g) Ma, S.; Zhang, J.; Chen, J.; Wang, L.; Xu, B.; Tian, W. *Chin. J. Chem.* **2013**, *31*, 1418; (h) Yoshii, R.; Nagai, A.; Tanaka, K.; Chujo, Y. *Chem. Eur. J.* **2013**, *19*, 4506; (i) Wang, Z.; Fang, Y.; Sun, J.; Qin, A.; Tang, B. Z. *Sci. China Chem.* **2013**, *56*, 1187; (j) Wang, X.; Wu, Y.; Liu, Q.; Li, Z.; Yan, H.; Ji, C.; Duan, J.; Liu, Z. *Chem. Commun.* **2015**, *51*, 784.
- [7] (a) Luo, Z. T.; Yuan, X.; Yu, Y.; Zhang, Q. B.; Leong, D. T.; Lee, J. Y.; Xie, J. P. *J. Am. Chem. Soc.* **2012**, *134*, 16662; (b) Liang, J. H.; Chen, Z.; Yin, J.; Yu, G. A.; Liu, S. H. *Chem. Commun.* **2013**, *49*, 3567; (c) Chen, Z.; Zhang, J.; Song, M.; Yin, J.; Yu, G.-A.; Liu, S. H. *Chem. Commun.* **2015**, *51*, 326.
- [8] (a) Zhang, Y.; Han, T.; Gu, S.; Zhou, T.; Zhao, C.; Guo, Y.; Feng, X.; Tong, B.; Bing, J.; Shi, J.; Zhi, J.; Dong, Y. *Chem. Eur. J.* **2014**, *20*, 8856; (b) Han, T.; Zhang, Y.; Feng, X.; Lin, Z.; Tong, B.; Shi, J.; Zhi, J.; Dong, Y. *Chem. Commun.* **2013**, *49*, 7049.
- [9] Satoh, T.; Ogino, S.; Miura, M.; Aromitra, M. *Angew. Chem., Int. Ed.* **2004**, *43*, 5063.

(Pan, B.; Qin, X.)